ELSEVIER

Oxide/hydroxide films on tin. Part I: Kinetic aspects of the electroformation and electroreduction of the films

V. Brunetti, M. López Teijelo *

*INFIQC, Departamento de Fisicoquímica, Facultad de Ciencias Químicas, Universidad Nacional de Córdoba,
Haya de la Torre y Medina Allende, 5000 Córdoba, Argentina*

Abstract

The anodic behaviour of tin in borate solutions has been studied by linear potential sweep voltammetry and triangularly modulated triangular potential sweeps. It is shown that the active to passive transition involves the formation of intermediate soluble species followed by the precipitation of a tin oxide/hydroxide layer that passivates the electrode. The potentiodynamic current-potential behaviour is adequately described by using the *Layer-pore-resistance model*. A good agreement between experimental and theoretical curves is obtained which allow us to demonstrate that primary passivation of tin in alkaline borate solutions (pH 8.9) as well as the film electroreduction is mainly controlled by the resistance of the electrolyte in the pores of the layer. In addition, the triangularly modulated triangular potential sweep method is applied in order to analyze the existence of reaction intermediates.
© 2007 Elsevier B.V. All rights reserved.

Keywords: Tin oxide; Passivating film; Ohmic resistance; Layer-pore-resistance model; Oxide/hydroxide film

1. Introduction

Oxide/hydroxide film formation during the anodic polarization of active metals is a relevant phenomenon in many electrochemical processes such as electrochemical machining, electrolytic polishing and pitting corrosion [1,2]. In particular, tin as a metal finds its most important applications in tin-plate and electronic industries [3].

The electrochemical behaviour of tin electrode in aqueous electrolytic solutions has been extensively studied mainly in alkaline solutions, and different mechanisms have been proposed for the active to passive transition [3–11] although some doubt still exists regarding the kinetics of the electroformation and electroreduction of the film. The primary passivation is considered that occurs as a consequence of the $Sn(OH)_2$ or SnO film formation by a dissolution-precipitation mechanism while the passive state is reached after the formation of a continuous film of $Sn(OH)_4$ by a solid state mechanism [3]. Then, the $Sn(OH)_4$ film can dehydrate to form more stable species like SnO_2 or $SnO_2 \cdot H_2O$ [3]. Some authors have suggested a duplex nature for the anodic film formed [9,12], consisting of a thick, poorly adherent and generally amorphous layer of $5SnO \cdot 2H_2O$ overlaying a thin, strongly adherent film of small crystals of $SnO_2 \cdot H_2O$.

Kapusta and Hackerman studied the passivation of tin under both potentiostatic and galvanostatic conditions [5–7]. In borate buffer, they reported anodic-charging curves similar to those observed on valve metals. Ammar et al. showed that the formation of anodic oxides on tin follow the same oxidation kinetics characteristic of valve metals not only in neutral solutions, but also in the acid and alkaline pH ranges [10,11]. Furthermore, based on the dependence of peak current and peak potential with scan rate in potentiodynamic experiments, Metikos et al. [8] found that the film formation process is under ohmic resistance control although under galvanostatic conditions they claim that anodic film growth occurs by an activation

---

* Corresponding author. Tel.: +54 351 4334169; fax: +54 351 4334188.
  E-mail address: mlopez@mail.fcq.unc.edu.ar (M. López Teijelo).

controlled ion conduction under the influence of a high electric field across the film. More recently, Gervasi et al. have studied anodic films formed on tin in carbonate–bicarbonate buffer, pH 8.9 [4] and reported that the principal defects contributing to ionic transport in the passive film during oxide growth are anion vacancies, and hence the oxide is expected to be an oxygen ion conductor.

Although in the last three decades special attention has been paid to the study of the reactions on tin electrodes and the main characteristics of the chemical species formed are known, there are several kinetic aspects that continue under discussion.

The main objective of this work is to present experimental results that enable one to gain a deeper insight into the kinetics of electroformation and electroreduction of tin oxide/hydroxide films formed up to 0 V (SHE) in aqueous borate solutions. The full current/potential data obtained by applying triangular potential sweeps are compared with theoretical curves calculated for the *Layer-pore-resistance model* (LPRM) for processes which are controlled by ohmic resistance. In addition, the *triangularly modulated triangular potential sweep (TMTPS)* method is applied in order to analyze the existence of reaction intermediates.

2. Experimental

The working electrode consisted of a polycrystalline tin rod (Koch-Light, 99.999% purity) of 8 mm diameter mounted in a Teflon holder which exposes a circular area of 0.50 cm^2. Before the experiments the electrode surface was abraded with emery paper, then polished mechanically with diamond paste (9 and 3 μm) dispersed with ethylene glycol on a nylon cloth (Buehler) and aluminas (1, 0.3 and 0.05 μm) on a polishing cloth (Microcloth, Buehler). Afterwards, the electrode was repeatedly cleaned with purified water, immersed in the solution and cathodized at −1.29 V for 10 min before the experiments.

The electrochemical measurements were performed in a conventional three-compartment electrolysis cell using a gold sheet as counterelectrode and an Hg/Hg$_2$SO$_4$/Na$_2$SO$_4$ (1 M) as reference electrode. Nevertheless, all potentials are referred to the standard hydrogen electrode (SHE).

Solutions of 0.0125 M Na$_2$B$_4$O$_7$ (pH 8.9) were prepared from AR chemicals and purified water (Milli Ro-Milli Q system). Measurements were performed at 25 °C under nitrogen gas saturation.

Electrochemical measurements were done by applying repetitive triangular potential sweeps (RTPS) between preset lower ($E_{s,c}$) and upper ($E_{s,a}$) switching potentials at different scan rates (v). Moreover, the *triangularly modulated triangular potential sweep (TMTPS) technique* was also used. This method is a powerful tool for studying reaction intermediates produced during the electrochemical reactions [13,14] and consists essentially of a triangular potential sweep at a low scan rate (base signal, $v_b = 0.050$ V s^{-1}) and a superimposed triangular potential modulation at a faster scan rate (modulation signal, v_m, between 5 and

40 V s^{-1}). The amplitude of the modulation signal (ΔE_m) is smaller than the amplitude of the base signal ($\Delta E_m = 0.1$ V).

3. Results and discussion

3.1. General electrochemical behaviour

Fig. 1 shows the potentiodynamic j/E response of a polycrystalline tin electrode in a borate solution (pH 8.9) obtained at 0.05 V s^{-1} by applying a single triangular potential sweep between the potential limits corresponding to the hydrogen and oxygen evolution reactions. The description of this voltammogram, which is shown for the sake of comparison, has already been made [3]. The positive scan exhibits two well defined anodic current peaks (I and II) at ca. −0.55 V and −0.36 V respectively, which have been associated with the formation of a hydrous tin oxide/hydroxide film [3]. At more positive potentials a wide potential region where a steady state current density is established (III), can be seen. This potential range corresponds to the film growth in the passive state. Also, a slight increase of the steady state current at potentials exceeding ca. 0.6 V is obtained. According to Kapusta et al. [3], peak I is assigned to the formation of a thin layer of either Sn(OH)$_2$ or SnO on the metal surface:

$$Sn + 2OH^- \rightarrow Sn(OH)_2 + 2e^- \qquad (1)$$
$$Sn + 2OH^- \rightarrow SnO + H_2O + 2e^- \qquad (2)$$
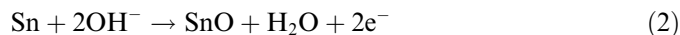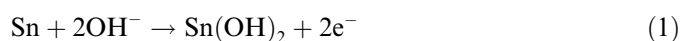
Then, this film is oxidized at more positive potentials (peak II):

$$Sn(OH)_2 + 2OH^- \rightarrow Sn(OH)_4 + 2e^- \qquad (3)$$
$$SnO + H_2O + 2OH^- \rightarrow Sn(OH)_4 + 2e^- \qquad (4)$$
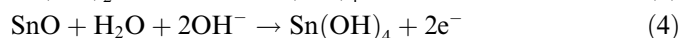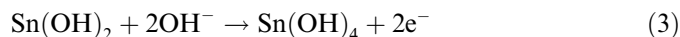
Finally, under anodic polarization the Sn(IV) hydroxide film dehydrates to form the more stable species, SnO$_2$ · H$_2$O [3].

The negative sweep shows a main cathodic peak at ca. −0.8 V (IV), which has been attributed to the electroreduction of the hydrous tin oxide/hydroxide film electroformed in the potential region of peaks I and II.
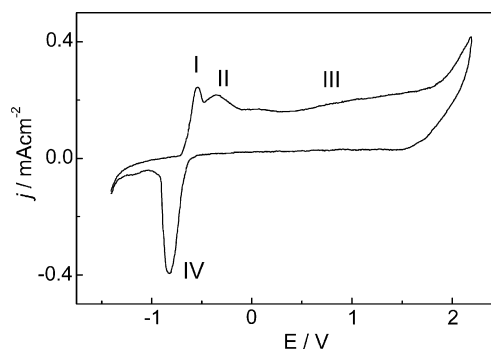

Fig. 1. Potentiodynamic j/E profile for Sn in borate solutions (pH = 8.9). $v = 0.050$ V s^{-1}.

In order to characterize the kinetics of electroformation and electroreduction of the tin oxide/hydroxide film in the potential region where the overall $Sn(0) \leftrightarrow Sn(IV)$ reaction takes place, the potentiodynamic j/E response obtained under different conditions is analyzed. Furthermore, the kinetic characteristics of tin oxide film growth in region III is described in Part II of this series.

Fig. 2 shows the electroreduction profiles obtained when the upper switching potential ($E_{s,a}$) is changed. As the switching potential becomes more positive, peak potential for the electroreduction process ($E_{p,c}$) shifts towards more negative values and the irreversibility of the overall redox process increases. The cathodic peak current density ($j_{p,c}$) first increases with the upper switching potential up to $E_{s,a} = 0$ V, afterwards a slight decrease of $j_{p,c}$ is observed and then the cathodic current peak remains almost constant. The inset in the figure shows the dependence of $E_{p,c}$ on $E_{s,a}$, which exhibits two clearly defined regions. The first region (up to $E_{s,a} = 0$ V) corresponds to the increase of the irreversibility of the overall electrochemical process in the primary passive region while the second region is probably related to changes in the layer structure and/or hydration, producing a change in the kinetics of growth of the oxide layer at potentials more positive than 0 V.

Fig. 3 illustrates the effect of sweep rate on the voltammetric profiles for both the oxidation and the reduction processes in the potential region between -1.2 V and -0.5 V where the first stages of electro-oxidation/electro-reduction (Eqs. (1),(2)) take place. In this potential region, even under repetitive scan conditions the voltammograms exhibit a poorly defined anodic current peak. Peak current density for both the anodic and the cathodic processes are scan rate (v) dependent and exhibit a nearly linear variation with $v^{1/2}$ as shown in Fig. 4a. Additionally, the peak potential for the anodic process does not show a simple relationship with scan rate while the corresponding value for the cathodic process, $E_{p,c}$, exhibits a linear dependence with log v with a slope of -60 mV/dec (Fig. 4b). These results suggest that the first process associated with the Sn(II) oxide/hydroxide formation, which leads to the tin primary passivation, is rather complex and may involve the forma-

Fig. 3. Potentiodynamic j/E profiles at different potential sweep rates in the potential region of peak I.

Fig. 4. (a) Dependence of $j_{p,a}$ and $j_{p,c}$ on $v^{1/2}$. (b) Dependence of $E_{p,c}$ on log v.

tion of soluble species while the electroreduction process is kinetically controlled [15].

On the other hand, Fig. 5 shows the effect of sweep rate on the quasi-stabilized voltammetric profiles obtained when the potential scan ($E_{s,a} = 0.2$ V) includes the overall two-stage tin oxide/hydroxide formation. Under these conditions, peaks I, II and IV are very well defined. In addition, it is clearly seen that the j/E curves have the same general shape at the different sweep rates. Furthermore, in the potential regions prior to the anodic and cathodic peaks, the current is independent of sweep rate and varies linearly with potential, exhibiting an ohmic behaviour. This type of response is characteristic of the formation of a layer under ohmic resistance control [16–18] where the
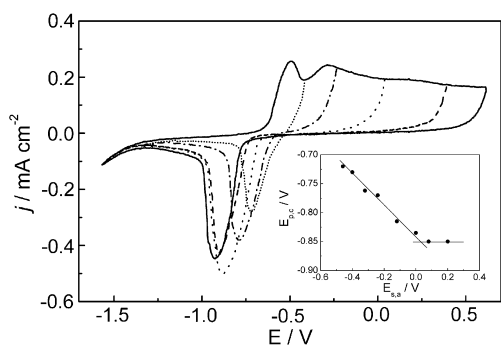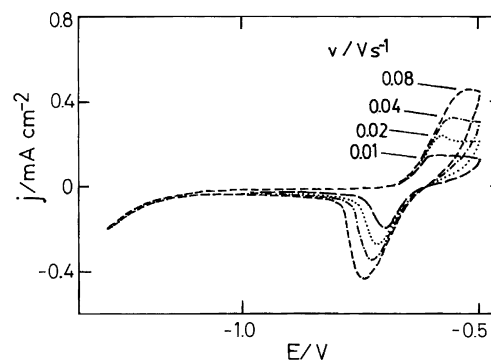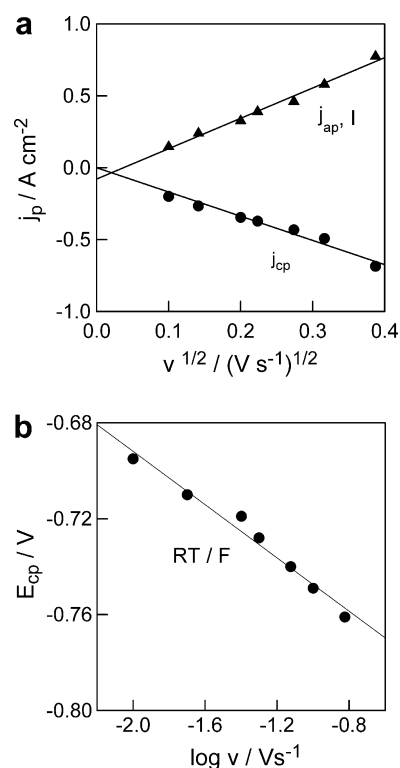

Fig. 2. Effect of the upper switching potential on the electroreduction j/E profiles. $v = 0.050$ V s^{-1}. Inset: dependence of $E_{p,c}$ on $E_{s,a}$.
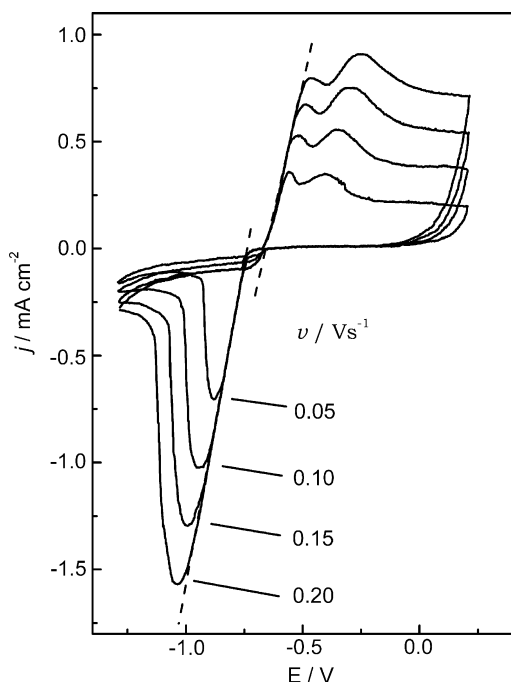
Fig. 5. Potentiodynamic j/E profiles at different potential sweep rates in the potential range covering peaks I and II. The dashed lines indicate the reciprocal of the overall resistance for the anodic and cathodic processes.

passivating oxide layer grows and spreads across the surface until only small pores in the layer remain and the overall rate is controlled by the resistance of the electrolyte in the pores.

3.2. Layer-pore-resistance model

The *Layer-pore-resistance model* (LPRM) can be used to explain the behaviour for the electrochemical cells in which the transient regime is controlled by a surface process. The growth of an insulating or poorly conducting film onto the electrode surface causes a change of the ohmic resistance during the layer electroformation. Then, the resistance of the layer-pore system is assumed to determine the rate of reaction.

From random nuclei, the passivating compound spreads over the electrode until only small pores in the layer remain. Thus, the passivating film acts as a mechanical barrier to the current flow, which is controlled by the resistance of the layer-pore system. If the total area of the electrode is A and θ is the degree of coverage of the surface, the resistance of the electrolyte in the pores $R\,(\theta)$ can be expressed in terms of the film thickness and the specific conductivity κ of the electrolyte [17] as

$$R(\theta) = \frac{d_0\theta^{1/2}}{\kappa A(1-\theta)} \qquad (5)$$

where d_0 is the maximum thickness. The resistance of a layer of electrolyte of thickness d_0 (b) can be written as:

$$b = \frac{d_0}{\kappa A} \qquad (6)$$

When an external potential E is applied to the system, the resulting current I depends on the total resistance which is given by the resistance $R\,(\theta)$ of electrolyte in the pores and the ohmic drop in the circuit excluding the surface process, R_0:

$$I = \frac{E}{R_0 + R(\theta)} \qquad (7)$$

The charge Q involved in the process depends on thickness and θ which are both time-dependent variables:

$$Q = \frac{zF\rho d_0 A}{M}\theta^{3/2} = Q_0\theta^{3/2} \qquad (8)$$

where ρ is the film density, M the molecular weight of the insoluble compound and Q_0 is the total charge required to cover the whole surface area with a film of thickness d_0.

According to the *Layer-pore-resistance model* (LPRM), the j/E curves should exhibit a maximum in current in which both j_p and E_p increase linearly with the square root of the potential sweep rate, provided that the coverage of the surface at the peak, θ_p, is independent of the scan rate. Fig. 6(a, b and c) shows the linear dependences of j_p and E_p vs. $v^{1/2}$ obtained for both anodic current peaks I and II and the cathodic current peak. The slope of the $j_p - v^{1/2}$ and $E_p - v^{1/2}$ plots depends on the properties and thickness of the film according to:

$$j_p = \left[\frac{3Q_o\theta_p}{b(1-\theta_p)}\right]^{1/2} (1-\theta_p)v^{1/2} \qquad (9)$$

$$E_p = \left[\frac{3Q_o\theta_p}{b(1-\theta_p)}\right]^{1/2} [R_o(1-\theta_p) + b\theta_p^{1/2}]v^{1/2} \qquad (10)$$

Moreover, a linear variation of E_p vs. j_p is also observed with a slightly different slope for each process (Fig. 6(d)). For the anodic film formation, the overall resistance derived from Fig. 6(d) is $\sim$7.1 Ω cm^2 for peak I and 8.6 Ω cm^2 for peak II while a value of $\sim$10 Ω cm^2 was obtained for the cathodic process.

In order to investigate the overall kinetic behaviour, the analysis of the whole information contained in the voltammograms is desirable. As a proof of the validity of the proposed model and to analyze the shape of the voltammograms, the j/E profiles run at different sweep rates are normalized dividing the current and the potential scales by the square root of sweep rate [18]. The normalized potential values are offset to zero in order to compare the shape of the voltammograms obtained at different v. Fig. 7 shows the normalized current/potential curves for the anodic process at different scan rates, taken from data of Fig. 5. It can be seen that peak I shows the same shape in these normalized scales while peak II presents changes in the shape that can be attributed to the increasing importance of other non-resistive processes like the further growth of the anodic oxide at more positive potentials, which are more important as the scan rate increases. The same analysis can be made for the cathodic peak, which corresponds to the overall electroreduction reaction
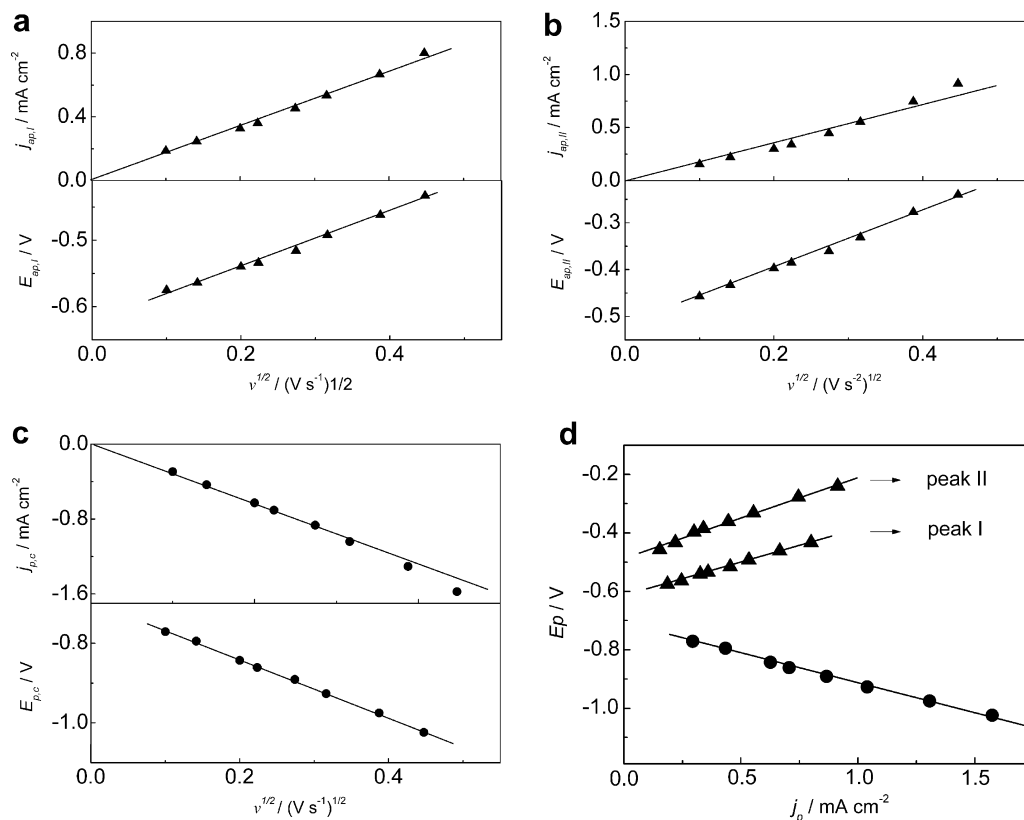
Fig. 6. (a) Dependence of $j_{ap,I}$ and $E_{ap,I}$ on $v^{1/2}$. (b) Dependence of $j_{ap,II}$ and $E_{ap,II}$ on $v^{1/2}$. (c) Dependence of j_{cp} and E_{cp} on $v^{1/2}$. (d) Dependence of E_p on j_p (▲) anodic and (●) cathodic processes.
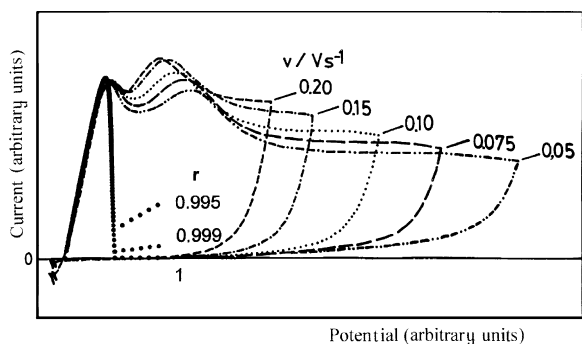

Fig. 7. Normalized j/E profiles for the anodic process (data of Fig. 5). (●) Calculated with the LPRM for films with different conductivities. $r = 1 - (\kappa_p/\kappa)$; ($r = 1$ insulating film).

Fig. 8. Normalized j/E profiles of the data of Fig. 5.

Sn(IV) → Sn (0). Fig. 8 shows the j/E curves in the normalized current and potential scales corresponding to the overall cathodic process at the different scan rates (Fig. 5). Identical j/E profiles are obtained in this case, indicating the suitability of the model. In addition, the value of the ohmic resistance is the same for all the sweep rates and that the overall rate is controlled by the resistance of the electrolyte in the pores.

Moreover, the potentiodynamic j/E response for films of different conductivities (κ_p) can be simulated using the LPRM as developed by Devilliers et al. [17] and compared
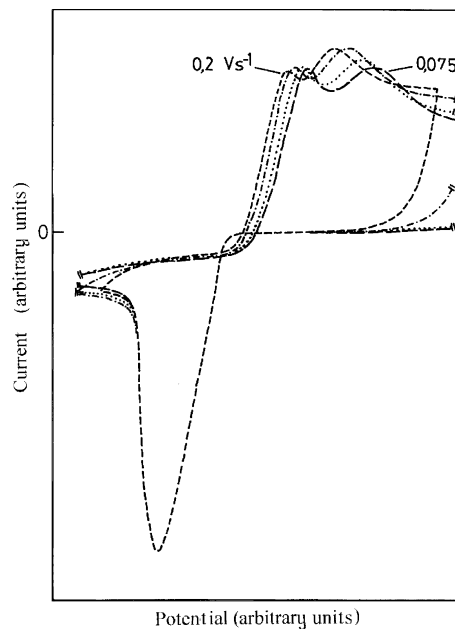
with the experimental results. Fig. 7 also shows the current/potential curves calculated in the potential region of peak I from the LPRM at different values of $r = 1 - (\kappa_p/\kappa)$, for an insulating film ($r = 1$) as well as for films showing some conductivity ($r < 1$). The agreement is good up to potential

values corresponding to E_p. At higher potentials, further oxidation to Sn(IV) species takes place (Eqs. (3),(4)) and peak II is obtained. This stepwise sequence of reactions precludes the quantitative analysis of the whole anodic profiles, although it can be concluded that peak II is also mainly controlled by ohmic resistance (see Fig. 6). As the current recorded in the voltammograms for each potential value is the sum of superimposed currents representing more than one phenomenon, we also tried to obtain the experimental separation of anodic peaks I and II following the approach proposed by Amaral et al. [19], although this procedure was unsuccessful in our case due to more than one electrochemical process was occurring simultaneously in the potential range under study.

Fig. 9 shows the cathodic curves obtained at different scan rates compared with those calculated according to the LPRM. Experimental values of charge were used in all calculations. The excellent agreement between the experimental data and the model indicates that the oxide/hydroxide electroreduction process is mainly controlled by the resistance of the electrolyte in the pores of the layer. At more negative potentials than ca. −1.6 V, deviations due to a cathodic current contribution of a second reduction process are observed. This second contribution would correspond to the layer of oxide which grows at more positive potentials and shows a more irreversible kinetic behaviour. Moreover, voltammograms may exhibit a second cathodic current peak when the oxide is grown at potentials more positive than 0.5 V [5].

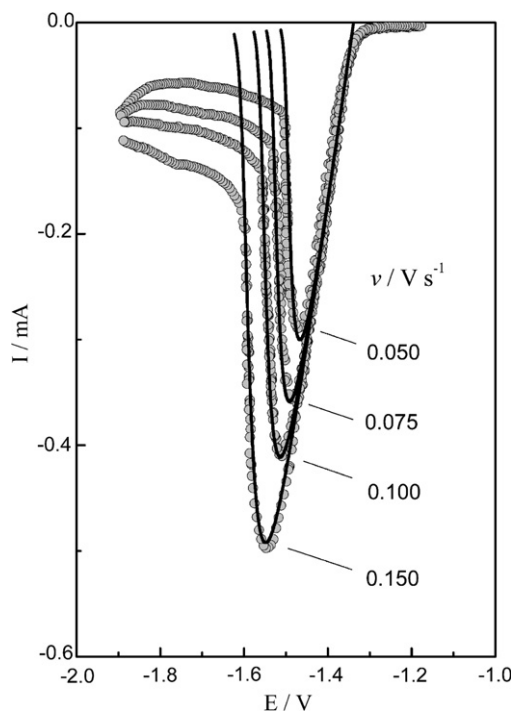Fig. 9. Potentiodynamic j/E curves for the electroreduction of the oxide formed up to 0.2 V at different sweep rates. (●) experimental (—) calculated with the LPRM for an insulating film using the experimental values of cathodic charge obtained from voltammograms.

3.3. Triangularly modulated triangular potential sweep experiments

In order to distinguish the kinetic response of intermediate species formed during the electrochemical reaction in different potentials region, the triangularly modulated triangular potential sweep (TMTPS) technique was used [13,14]. The modulation allows the detection of intermediate species as the base signal moves in the positive or negative directions. The overall j/E response depends on the scan rate of both signals (base and modulation) as well as the modulation signal amplitude. The TMTPS response obtained in the potential region corresponding to the anodic current peak I (from ca. −0.7 V up to −0.6 V), exhibits an anodic current contribution similar to the cathodic current for both the positive and the negative scans and the overall profiles show a remarkable reversibility (see supplementary data). The response in this potential region may be related to the reversible reaction of intermediate OH species adsorption on the metal which takes place during the initial stages of the film formation. Similar results for anions adsorption/desorption on Cu [20] and Fe [21] in alkaline media have been reported. As the upper switching potential is increased ($E_{s,a} = -0.5$ V), the resistive contribution becomes evident. The increasing current regions for both the positive and the negative scans show a linear j/E dependence. The j/E displays exhibit an anodic current greater than the cathodic current at the positive scan while the opposite occurs during the negative scan, indicating also an increasing irreversibility (see supplementary data).

Moreover, the negative scan shows a broad anodic current peak at −0.67 V and a shoulder at −0.7 V, suggesting that two current contributions are present in this potential region. When the scan rate of the modulation signal is increased, the two anodic contributions during the negative sweep corresponding to the two-step anodic reaction are clearly defined (see supplementary data). Also, the capacitive current contribution is more important in this case. These results indicate that, under the present experimental conditions, the overall anodic reaction occurs by a two-step path which is related to the Sn(II) and Sn(IV) species formation, while the film electroreduction occurs through a one-stage Sn(IV) → Sn(0) overall reaction. Both processes are mainly controlled by ohmic resistance of electrolyte in the pores.

4. Conclusions

The kinetic characteristics during the electroformation and electroreduction of tin oxide/hydroxide films formed in aqueous borate solutions up to 0 V (SHE) have been obtained. The analysis of the potentiodynamic measurements (RTPS and TMTPS) suggest that tin passivation in alkaline media takes place by a complex mechanism which includes several steps. At the initial stages of the Sn(II) oxide/hydroxide film formation, a reversible process that

can be attributed to the formation of intermediate OH species on the metal surface, is observed. Then, the primary passivation occurs due to the precipitation of a poorly conducting layer of SnO or $Sn(OH)_2$. This primary passive layer is further oxidized to $Sn(OH)_4$, which after a dehydration process to produce a SnO_2 layer, grows as a continuous film by a solid state mechanism. The data obtained by repetitive triangular potential sweeps compared with theoretical curves for the *Layer-pore-resistance model* (LPRM), demonstrate that both the oxide electroformation and electroreduction processes are controlled by ohmic resistance. First, the passivating layer grows and spreads across the surface until only small pores in the layer remain and the overall rate is controlled by the resistance in the pores. Then, a continuous film is formed at potentials more positive than 0 V presenting a change in the kinetics of growth which will be analyzed in Part II of this series [22].

Acknowledgements

Appendix A. Supplementary data

Supplementary data associated with this article can be found, in the online version, at doi:10.1016/j.jelechem.2007.10.002.

References

[1] D.F.A. Koch, in: J.O.M. Bockris, B.E. Conway (Eds.), Modern Aspects of Electrochemistry, vol. 10, Plenum Press, New York, 1975, Chapter 4.
[2] V.I. Birss, G.A. Wright, Electrochim. Acta 26 (1981) 1809–1817.
[3] S.D. Kapusta, N. Hackerman, Electrochim. Acta 25 (1980) 1625–1639.
[4] C.A. Gervasi, P.E. Alvarez, Corros. Ser. 47 (2005) 69–78.
[5] S.D. Kapusta, N. Hackerman, Electrochim. Acta 25 (1980) 949–955.
[6] S.D. Kapusta, N. Hackerman, Electrochim. Acta 25 (1980) 1001–1006.
[7] S.D. Kapusta, N. Hackerman, Electrochem. Soc. 129 (1982) 1886–1889.
[8] M. Metikos-Hukovic, A. Resetic, V. Gvozdic, Electrochim. Acta 40 (1995) 1777–1779.
[9] M. Metikos-Hukovic, M. Seruga, F. Ferina, Ber. Bunsenges. Phys. Chem. 96 (1992) 799–805.
[10] A. Ammar, S. Darwish, M.W. Khalil, S. El-Taher, Electrochim. Acta 33 (1988) 231–238.
[11] I.A. Ammar, S. Darwish, M.W. Khalil, S. El-Taher, Corrosion 46 (1990) 197–202.
[12] R.O. Ansell, T. Dickinson, A.F. Povey, S. Sherwood, Electrochem. Soc. 124 (1977) 1360–1364.
[13] B.E. Conway, H. Angerstein-Kozlowska, F.C. Ho, J. Klinger, B. MacDougall, S. Gottesfeld, Discuss. Faraday Soc. 56 (1973) 210–227.
[14] N.R. Tacconi, J.O. Zerbino, A.J. Arvia, J. Electroanal. Chem. 79 (1977) 287–292.
[15] D.D. Macdonald, Transient Techniques in Electrochemistry, Plenum Press, New York and London, 1977, Chapter 8.
[16] A.J. Calandra, N.R. Tacconi, R. Pereiro, A.J. Arvia, Electrochim. Acta 19 (1974) 901–905.
[17] D. Devilliers, F. Lantelme, M. Chemla, Electrochim. Acta 31 (1986) 1235–1245.
[18] V. Brunetti, H.M. Villullas, M. López Teijelo, Electrochim. Acta 44 (1999) 4693.
[19] S.T. Amaral, E.M.A. Martín, I.L. Müller, Corros. Sci. 43 (2001) 853–879.
[20] M.J. Dignam, D.G. Gibbs, Canadian J. Chem. 48 (1970) 1242.
[21] H. Worch, W. Forker, Electrochim. Acta 35 (1990) 163.
[22] V. Brunetti, M. López Teijelo, J. Electroanal. Chem. 613 (2008) 16–22.